Internal photopolarization effect in asymmetric superlattices

Serge Luryi and Chun-Ting Liu
AT&T Bell Laboratories, Murray Hill, New Jersey 07974
(Received 24 April 1991)

We propose a steady-state photogalvanic effect in semiconductor superlattices lacking reflection symmetry. The effect arises when the average generation and recombination events are spatially displaced from one another. In the steady state, this requires an internal current of majority carriers and a voltage driving that current. The resultant polarization of the superlattice is a tangible effect, provided the minority-carrier lifetime is sufficiently short, and it can be used to control the gate of a field-effect transistor. The described effect is likely to generate useful applications, especially for fiber-optic communications.

I. INTRODUCTION

Several years ago, Capasso *et al.*[1] described a transient electrical polarization phenomenon in sawtooth superlattices. They used a *p*-type-doped graded-gap $Al_{1-x}Ga_xAs$ sawtooth structure, cf. Fig. 1. In such structures the valence band is flat, tied to the equilibrium Fermi level, while the conduction band appears graded. Sudden illumination of the structure by high-energy photons gives rise to a substantial voltage across the superlattice, which then rapidly decays, so that the effect is essentially transient. No steady-state polarization has been observed under dc illumination.

In the present paper we reanalyze the behavior of asymmetric superlattices under illumination and show that certain structure parameters can be modified so that a *steady-state* polarization will be induced by light. This effect will persist so long as the structure is illuminated and, as the light is turned off, it will disappear. We shall show that both the rise and the fall of the light-induced steady-state polarization are determined by extremely fast processes, so that the structure can be operated as a detector with a picosecond response. A unique property of this type of detector is that it can be operated with a capacitive load, permitting a natural integration with a field-effect transistor (FET).

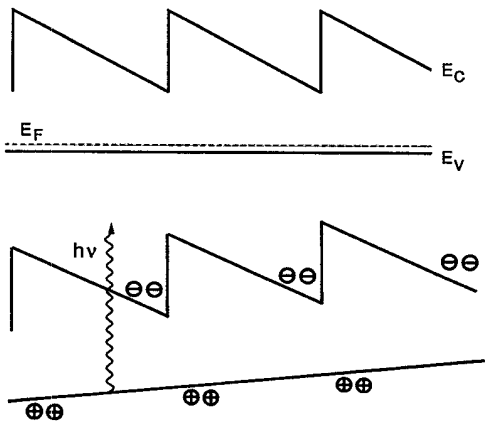

FIG. 1. Sawtooth in equilibrium and under illumination (after Ref. 1).

The transient effect arises when the electron transit time τ_d across one superlattice period d is shorter than the Maxwell relaxation time τ_M of the *p*-type-doped material. An abrupt light pulse generates electron-hole pairs and sets electrons in motion that temporarily upsets the local balance of charge. Because of the sawtooth asymmetry, the polarization from each period adds up like in a pyroelectric, developing a voltage across the superlattice. The rise time of the transient polarization effect is of order τ_M.

The transient effect is practically independent of the minority-carrier lifetime τ_e, because the recombination of an electron with a hole does not change the charge distribution and leaves the photovoltage unaffected. In contrast, for the steady-state effect discussed in the present work the minority lifetime is the most important parameter. The absence of a steady-state polarization in the experiments[1] will be explained by the fact that τ_e was insufficiently short.

Like the transient effect, the electrical polarization under dc illumination arises owing to the lack of a reflection symmetry in the superlattice. In a steady state, the generation of electron-hole pairs is (approximately) uniform over the entire structure, while the recombination occurs predominantly at the narrow-band end of the superlattice period, where the minority-carrier concentration is highest. A steady-state supply of the majority carriers must be provided by a gradient of their quasi-Fermi level, $E_{F,h}$, which drags the necessary amount of holes toward the narrow-band-gap region of the superlattice. In the absence of an external current, the electron and hole fluxes are equal at every point. Because of the sawtooth asymmetry, the electron current is almost everywhere directed along the conduction-band gradient and this ensures a unidirectional nature of the hole flow. Hence a nonvanishing hole quasi-Fermi-level difference eV_1 is generated in each period. These differences add up to a finite voltage V between the top and the bottom layers of the superlattice.

The described effect may be compared to the well-known photodiffusion (Dember) effect,[2] in which the

generation of electron-hole pairs occurs in a small part of the sample, adjacent to an illuminated surface, while their recombination spreads over a larger distance corresponding to the ambipolar diffusion length. The Dember effect is relatively slow, being controlled by the minority carrier storage. In contrast, the present effect is much faster: both the rise time, after the incident radiation is turned on, and its fall time, after the radiation is turned off, are described by the Maxwell relaxation time τ_M which can be in the subpicosecond range. The Dember field is proportional to the difference of the diffusion coefficients of electrons (D_e) and holes (D_h), whereas the polarization field discussed in the present work is insensitive to this difference and does not vanish when $D_e = D_h$.

Let us discuss why the steady-state effect has not been seen experimentally. It is clear that under dc conditions the polarization voltage is proportional to the radiation intensity and inversely proportional to the hole conductivity. Simple calculation, presented in the next section, gives

$$V = NV_1 = \frac{NGd^2}{2\mu_h p_0} \approx \frac{\Phi d}{2\mu_h p_0} , \tag{1}$$

where Φ is the photon flux ($\text{cm}^{-2}\,\text{sec}^{-1}$), N the number of superlattice periods, $G \equiv \alpha\Phi$ the generation rate, α the absorption coefficient (assumed uniform), μ_h the hole mobility, and p_0 the uniform hole concentration provided by doping. The last form in the right-hand side of (1) is obtained by assuming that the superlattice is thick enough ($\alpha Nd \sim 1$) to absorb most of the incident radiation. It may appear that a sufficiently high illumination intensity can always bring V into a measurable range, at least in low-doped samples. However, increasing the generation rate G beyond p_0/τ_e, does not lead to a higher photovoltage. Indeed, for $G\tau_e > p_0$, the hole conductivity itself becomes proportional $G\tau_e$, and the photovoltage (1) will saturate,

$$V \approx \frac{NGd^2}{2\mu_h(p_0 + G\tau_e)} \lesssim V_{\max} = \frac{Nd^2}{2\mu_h\tau_e} . \tag{2}$$

If we assume a relatively low value of the hole mobility, $\mu_h \sim 100$ $\text{cm}^2/\text{V sec}$, parameters of the experiment,[1] $d = 500$ Å and $N = 10$, and a lifetime limited by the radiative recombination in a low-doped GaAs, $\tau_e \sim \tau_r \gtrsim 10^{-8}$ sec, then the maximum voltage predicted by Eq. (2) is $V_{\max} \sim 10^{-4}$ V, which is too low to have been noticed.

However, τ_e does not have to be that long. Free-carrier lifetimes as low as 1 psec have been demonstrated in radiation-damaged photoconductors.[3–5] Moreover, the lifetime need not be uniform. One can envisage a possibility of "lifetime engineered" structures with $\tau_e(x)$ designed so as to enhance the steady-state polarization effect. It can also be done "with the mirrors," providing for a stimulated recombination in a portion of the superlattice period. With a sufficiently short recombination time, the polarization voltage attains respectable values that may be used in applications. We can expect that for a practical use, the voltage generated per period should be of order 10 mV or higher, resulting in the overall voltage V of a few tenths of a volt. As will be shown below, these are certainly achievable numbers and it is, therefore, reasonable to consider useful devices based on this principle.

This paper is organized as follows. In Sec. II we derive Eq. (1) for the sawtooth superlattice (and similar equations for other asymmetric structures) from a rigorous transport model, based on the drift-diffusion equation. Examples considered include not only band-gap-engineered superlattices but also structures with nonuniform τ_e. In Sec. III, we consider the situations when a steady-state-polarized superlattice is shunted by a resistor or shares its charge with an external capacitor. Transient processes are also discussed and an equivalent circuit model is presented. Even though the results obtained are quite simple, they are worth discussing because the behavior of a nonequilibrium pyroelectric under load is not intuitively obvious. Section IV deals with an idealized integrated structure in which the photopolarized superlattice is electrically connected between the source and the gate of a FET. This analysis permits us to establish the limits of performance of such systems and demonstrates the existence of a tradeoff between their efficiency and speed of response.

II. EVALUATION OF THE STEADY-STATE PHOTOPOLARIZATION

In this section the steady-state polarization will be evaluated for several possible device structures (Fig. 2) under open-circuit conditions. The situation under load, capacitive or resistive, will be considered in Sec. III. In an open circuit, the total current vanishes in the steady state,

$$\mathbf{J} = \mathbf{J}_e + \mathbf{J}_h = 0 , \tag{3}$$

where $\mathbf{J}_e$ and $\mathbf{J}_h$ are the densities of the electron and the hole currents, respectively.

Carrier transport will be described by the drift-diffusion equations,

$$\mathbf{J}_e = n\mu_e \nabla E_C + eD_e \nabla n , \tag{4a}$$

$$\mathbf{J}_h = p\mu_h \nabla E_V - eD_h \nabla p , \tag{4b}$$

where n is the electron density and μ_e, D_e are, respectively, the electron mobility and diffusivity. The corresponding quantities for holes are p, μ_h, and D_h. The energy E_C designates the bottom of the conduction band and E_V the top of the valence band. Carrier concentrations are governed by the continuity equations

$$\frac{1}{e}\nabla\cdot\mathbf{J}_e + G - R = \frac{\partial n}{\partial t} = 0 , \tag{5a}$$

$$-\frac{1}{e}\nabla\cdot\mathbf{J}_h + G - R = \frac{\partial p}{\partial t} = 0 . \tag{5b}$$

We shall take $G = \alpha\Phi$ uniform over the superlattice period ($\alpha d = \text{const} \ll 1$), which is a reasonable assumption if the photon energy exceeds the fundamental threshold at the wide-gap end. The recombination term R will be assumed in the form

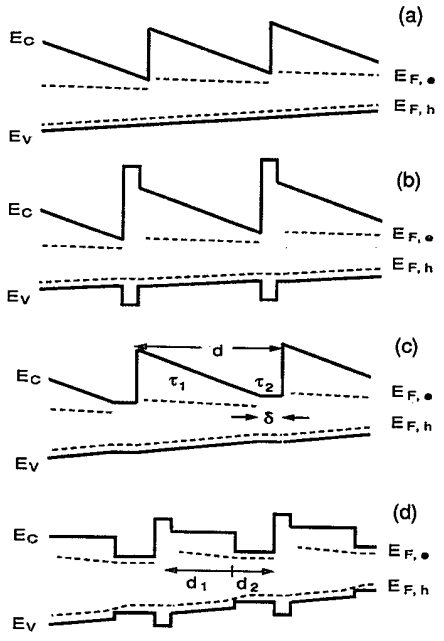

FIG. 2. Various asymmetric superlattices subject to a steady-state photopolarization: (a) conducting sawtooth, (b) sawtooth with barrier separators, (c) sawtooth with nonuniform τ_e, and (d) castellated superlattice.

$$R=\frac{n(x)}{\tau_e}\ , \tag{6}$$

where τ_e is the electron lifetime in the p-type material. We shall first consider the case of a spatially uniform τ_e.

A. Sawtooth superlattices: uniform lifetime

For a uniform $\tau_e \neq \tau_e(x)$, Eqs. (4a), (5a), and (6) reduce to a simple differential equation with constant coefficients

$$\frac{\partial^2 n}{\partial x^2}-\frac{eF}{kT}\frac{\partial n}{\partial x}-\frac{n}{D_e\tau_e}+\frac{G}{D_e}=0\ , \tag{7}$$

where $eF\equiv|\nabla E_C|$. In the derivation of this equation it has been assumed that F is constant, i.e., we have neglected the effect of the space-charge $\rho=\epsilon\nabla\cdot\nabla E_C$. As will be shown at the end of Sec. IV [cf. Eq. (34)], this charge is indeed small, $\rho \ll ep_0$, even at the highest illumination intensities, $G\sim p_0/\tau_e$. The general solution of Eq. (7) is of the form

$$n(x)=C_1e^{\gamma_1 x}+C_2e^{\gamma_2 x}+G\tau_e\ , \tag{8}$$

where

$$\gamma_1 d=\frac{1}{2\theta}+\frac{1}{2\theta}(1+4\theta^2d^2/\tau_eD_e)^{1/2}\approx\frac{1}{\theta}\left[1+\frac{\theta^2d^2}{\tau_eD_e}\right]\ , \tag{9a}$$

$$\gamma_2 d=\frac{1}{2\theta}-\frac{1}{2\theta}(1+4\theta^2d^2/\tau_eD_e)^{1/2}\approx-\frac{\theta d^2}{\tau_eD_e}\ , \tag{9b}$$

and

$$\theta\equiv\frac{kT}{eFd}=\frac{Kt}{\Delta}\ . \tag{10}$$

We shall assume $d\approx10^{-5}$ cm and $\Delta\gtrsim0.25$ eV, so that at room temperature, $\theta\sim0.1$. It is the basic small parameter in the problem.

Using the fact that $\gamma_1+\gamma_2=1/\theta d$, we can bring the expression for the electron current into a compact form

$$-\frac{J_e(x)d}{eD_e}=C_1(\gamma_2 d)e^{\gamma_1 x}+C_2(\gamma_1 x)e^{\gamma_2 d}+\frac{G\tau_e}{\theta}\ . \tag{11}$$

The coefficients C_1 and C_2 are determined from the boundary conditions at $x=0$ and $x=d$. In a structure with wide-gap barriers separating the graded-gap regions [Fig. 2(b)], the appropriate boundary conditions are

$$J_e(0)=J_e(d)=0\ , \tag{12}$$

whence we find

$$C_1=\frac{GD_e\tau_e^2}{\theta d}\frac{\gamma_1-\gamma_1e^{\gamma_2 d}}{e^{\gamma_1 d}-e^{\gamma_2 d}}\approx\frac{G\tau_e}{\theta}\left[1+\frac{\theta^2d^2}{\tau_eD_e}\right]e^{-\gamma_1 d}\ , \tag{13a}$$

$$C_2=\frac{GD_e\tau_e^2}{\theta d}\frac{\gamma_2e^{\gamma_1 d}-\gamma_2}{e^{\gamma_1 d}-e^{\gamma_2 d}}\approx-G\tau_e\left[1-\frac{\theta^2d^2}{\tau_eD_e}\right]\ . \tag{13b}$$

The boundary condition of vanishing electron current is not strictly valid for simple sawtooth structures [Fig. 2(a)] without barrier separators. A small thermionic flux of electrons is flowing in the direction opposite to the electron drift. However, from the analysis[6] of the thermionic and diffusion theories of barrier transport, we know that neglect of this current will introduce an error δn in the electron concentration at the top of the barrier that scales with θ as $\sim e^{-1/\theta}$. Such an error can be neglected.

Expanding the exact expressions (8) and (11) in powers of θ and neglecting terms of order θ^2, we find

$$n(x)=G\tau_e\frac{\Delta}{kT}\exp\left[-\frac{\Delta}{kT}\left[1-\frac{x}{d}\right]\right]+\frac{Gx}{\mu_eF}\ , \tag{14}$$

$$J_e(x)=eGd\exp\left[-\frac{\Delta}{kT}\left[1-\frac{x}{d}\right]\right]-eGx\ . \tag{15}$$

Writing the hole current (4b) in the form $\mathbf{J}_h=p\mu_h\nabla E_{F,h}$ and using Eq. (3), we have

$$V_1\equiv V(0)-V(d)=\frac{\Delta E_{F,h}}{e}=-\int_0^d\frac{J_e(x)dx}{ep\mu_h}\ . \tag{16}$$

Integrating Eq. (16), assuming a constant $p=p_0$, and dropping the term of order $e^{-1/\theta}$, we obtain

$$V_1=\frac{Gd^2}{2p_0\mu_h}\left[1-\frac{2kT}{\Delta}\right]\ , \tag{17}$$

which agrees with (1) to the lowest order in θ. It is clear that the result (17) is valid only if the density of photo-

generated carriers is less than p_0. For $G \approx p_0/\tau_e$, the second term in (14) is still small because, typically, $d \ll \mu_e F \tau_e$. The first term varies exponentially and, for $G \approx p_0/\tau_e$, it remains small over a fraction ξ of the period, determined by the inequality

$$\theta e^{(1-\xi)/\theta} > 1 . \tag{18}$$

In our exemplary case of $\theta \approx 0.1$, this inequality is satisfied for $\xi < 0.77$, i.e., the integration of Eq. (16) with $p = p_0$ is valid in more than half of the period. It is reasonable, therefore, to take $G = \tau_e^{-1} p_0$ as a watershed value at which the photovoltage V_1 saturates, i.e.,

$$V_1^{\max} \approx \frac{d^2}{2\mu_h \tau_e} , \tag{19}$$

in accordance with Eq. (2).

B. Sawtooth superlattices: nonuniform lifetime

The lifetime of minority electrons is determined by the doping concentration and other factors, such as the presence of neutral impurities and crystal defects, as well as, under certain conditions, by stimulated radiative recombination. In certain applications it may be advantageous to use a nonuniform $\tau_e(x)$. We shall consider here the simplest (and practically most reasonable) case of a piecewise nonunformity [Fig. 2(c)]

$$\tau_e = \begin{cases} \tau_1 & \text{if } 0 < x < d-\delta \\ \tau_2 & \text{if } d > x > d-\delta, \end{cases} \tag{20}$$

with $\tau_2 \ll \tau_1$. Even for a small δ, we shall require $\tau_2 \ll (\delta/d)\tau_1$, so that the recombination in the τ_1 region can be neglected.

Equations (4a), (5a), and (6) then reduce to a differential equation of the form

$$\frac{\partial^2 n}{\partial x^2} - \frac{eF}{kT}\frac{\partial n}{\partial x} + \frac{G}{D_e} = 0 \quad \text{for } x \le d-\delta , \tag{21}$$

with boundary conditions set at $x=0$ by $J_e = 0$ and at $x = d$ by

$$G\tau_2 d = \int_{d-\delta}^{d} n(x)dx \approx n(d)\delta . \tag{22}$$

Solving Eq. (21), we obtain the carrier concentration in the form

$$n(x) = \frac{Gd}{\mu_e F}\left[\frac{x}{d} + \theta + \frac{\mu_e F \tau_2}{\delta}\left(1 - \frac{\delta(1+\theta)}{\mu_e F \tau_2}\right) \times e^{(eF/kT)(x-d)}\right] . \tag{23}$$

To calculate the current in this case, there is no need to use Eqs. (4a) and (23). In the region where the recombination is neglected, the electron current density obviously equals

$$J_e(x) = -eGx \quad \text{for } x \le d-\delta , \tag{24}$$

as, of course, also follows from (23). The resulting polarization voltage,

$$V_1 \approx \frac{Gd(d-\delta)}{2p_0\mu_h} , \tag{25}$$

is similar to (1), but $V_1^{\max}$ in this case is not limited by the value of V_1 at $G = p_0/\tau_1$. Indeed, as seen from (23), the highest concentration n in the region $x \lesssim d-\delta$ is given by $G\tau_2(d/\delta)$, which is much lower than $G\tau_1$. Thus, under our assumption that $\tau_2 \ll (\delta/d)\tau_1$, the maximum polarization voltage is

$$V_1^{\max} = \frac{d\delta}{2\mu_h \tau_2} \gg \frac{d^2}{2\mu_h \tau_1} . \tag{26}$$

C. "Castellated" superlattices

In certain heterostructure materials, graded-gap sawtooth superlattices are difficult to achieve within the confines of lattice-matched heteroepitaxy. As we shall show now, the built-in sawtooth field is not a necessary requirement for the steady-state polarization effect. Consider the superlattice, illustrated in Fig. 2(d). Conduction band profiles of such shape will be referred to as "castellated." We shall assume that under illumination the conduction band is flat, as shown in the figure. This assumption implies a small built-in field in equilibrium. If such a field does not exist, then there must be a reverse field under illumination. We can safely neglect this field in the dynamics of the minority carriers if the total polarization voltage V_1 per period is sufficiently small: $\Delta E_{F,h} < kT$, a limit we do not aspire to reach in castellated superlattices.

For the sake of generality, we shall assume that the wide-gap portion d_1 of the period is characterized by the electron diffusivity D_1 and lifetime τ_1, and that the corresponding parameters in the narrow-gap part are D_2 and τ_2, respectively. The continuity equation for the minority current in this case reduces to

$$\begin{aligned} &n'' - n/\lambda_1 + G/D_1 = 0, \quad x < 0, \\ &n'' - n/\lambda_2 + G/D_2 = 0, \quad x > 0, \end{aligned} \tag{27}$$

where $\lambda_i^2 \equiv D_i \tau_i$ $(i = 1,2)$, and the origin $(x=0)$ is placed at the band discontinuity. The concentration $n(x)$ is no longer continuous at $x=0$, but the electron current density $J_e(x)$ and the quasi-Fermi level $E_{F,e}(x)$ will be assumed continuous. (The former of these assumptions means that we neglect surface recombination at $x=0$, the latter expresses our neglect of carrier heating or cooling on crossing the interface, which would violate a thermal equilibrium between adjacent points.)

The general solution of Eq. (27) can be written in the form

$$n(x) = G\tau_i + P_i \sinh(x/\lambda_i) + Q_i \cosh(x/\lambda_i) , \tag{28}$$

$$J_e(x) = (eD_i/\lambda_i)[P_i \cosh(x/\lambda_i) + Q_i \sinh(x/\lambda_i)] , \tag{29}$$

where we take $i=1$ for $x \le 0$ and $i=2$ for $x \ge 0$. The coefficients P_i and Q_i are found from the following four equations:

$$(D_1/\lambda_1)P_1=(D_2/\lambda_2)P_2\ , \tag{30a}$$

$$\frac{G\tau_1+Q_1}{G\tau_2+Q_2}=e^{\Delta/kT}\ , \tag{30b}$$

$$P_1/Q_1=\tanh(d_1/\lambda_1)\ , \tag{30c}$$

$$P_2/Q_2=-\tanh(d_2/\lambda_2)\ , \tag{30d}$$

which follow from the current continuity (30a), the quasi-Fermi level continuity (30b), and the boundary condition of vanishing current between different periods [(30c) and (30d)]. The result is

$$P\equiv\frac{G\lambda_1-G\lambda_2e^{\Delta/kT}(D_1\lambda_2/D_2\lambda_1)}{\coth(d_1/\lambda_1)+\coth(d_2/\lambda_2)e^{\Delta/kT}(D_1\lambda_2/D_2\lambda_1)}$$

$$\approx -Gd_2\ , \tag{31a}$$

$$P_i=(\lambda_i/D_i)P\approx -Gd_2\sqrt{\tau_i/D_i},\quad i=1,2, \tag{31b}$$

$$Q_i=P_i\coth(d_i/\lambda_i)\approx(-1)^iG\tau_i(d_2/d_i),\quad i=1,2, \tag{31c}$$

whence the current density is given by

$$\frac{J_e(x)}{e}=P[\cosh(x/\lambda_i)-(-1)^i\coth(d_i/\lambda_i)\sinh(x/\lambda_i)]$$

$$\approx -Dd_2[1-(-1)^i(x/\lambda_i)],\quad i=1,2\ . \tag{32}$$

The approximate expressions in the right-hand side of these equations are obtained under the further assumptions of a large band discontinuity, $\exp(\Delta/kT)\gg\tau_1/\tau_2$, and a large diffusion length, $\lambda_i\gg d_i$ $(i=1,2)$. The former of these additional assumptions determines the *direction* of the electron current: had we assumed $\exp(\Delta/kT)\ll\tau_1/\tau_2$, the value of the parameter P would be $P\approx+Gd_1$ and the electron flux would be directed from the narrow-gap into the wider-gap region. This would not be an unreasonable design: one can even take $\Delta=0$ and obtain the required asymmetry of the superlattice in virtue of only $\tau_1\gg\tau_2$. Our result shows that the lifetime engineering in the present context is just as powerful as the band-gap engineering.

Integrating Eq. (32), we find

$$V_1\approx\frac{Gdd_2}{2p_0\mu_h}\ , \tag{33}$$

which is not very different from the sawtooth case.

Finally, let us return to the space charge ρ, neglected throughout this section, and justify this neglect that had allowed us to let the field $F=\text{const}$ in Eqs. (7) and (21). The space charge ρ is the source of the electrostatic field in the photopolarized state. It represents a local disbalance of electrons, holes, and acceptors, $e(p-p_0)-en=\rho(x)$. An estimate for the peak magnitude of this charge can be obtained from Poisson's equation, viz., $eV_1/d\approx|\rho|d/2$, whence we find, using Eq. (17),

$$|\rho|\lesssim\frac{ep_0\tau_M}{\tau_e}\ . \tag{34}$$

This inequality shows that in the limit $\tau_M\ll\tau_e$, assumed throughout this work, we are entirely justified in neglecting the space charge ρ.

III. PHOTOPOLARIZED STRUCTURE UNDER LOAD; EQUIVALENT CIRCUIT MODEL

In this section we consider the transient and the steady-state response of asymmetric superlattices both in an open circuit configuration and under load. This discussion will lead us to an equivalent circuit model of the device, adequate for intended applications.

A. Transient response in an open circuit

Consider the intrinsic response time of the photopolarization effect. What happens when one of the structures discussed in Sec. II is illuminated by a "rectangular" light pulse, $G(t)=Gu(t)-Gu(t-t_p)$, where $u(t)$ is the unit step function and t_p the pulse duration. As we know from the experiment,[1] the leading edge of the pulse will be accompanied by a transient polarization, whose peak magnitude is independent of the minority lifetime τ_e. The transient voltage grows for the time of order τ_M determined by the Maxwell dielectric relaxation of the p-type-doped material,

$$\tau_M=\epsilon/e\mu_hp_0\ . \tag{35}$$

By the time $t\approx\tau_M$, the transient voltage begins to decline. For $\mu_h\approx100$ cm^2/V sec and $p_0=6\times10^{16}$ cm^{-3}, this time is $\tau_M\approx1$ psec. If the duration of the pulse is sufficiently long, $t_p\gg\tau_M$, then a steady state will be reached, described by the polarization voltage (2).

It may appear that the rise time of the transient polarization corresponds to an electron transit τ_d across one superlattice period d. This is not so. For a short $d\lesssim1000$ Å, we can estimate τ_d, assuming a ballistic flight

$$\tau_d=(md^2/\Delta)^{1/2}\lesssim10^{-13}\,\text{sec}\ , \tag{36}$$

where $\Delta\approx0.25$ eV is the total conduction-band energy drop across one period, and the effective mass of electrons in GaAs is assumed in the estimate. Suppose, therefore, that $\tau_d\ll\tau_M$. In this case, the polarization of the structure will be initially controlled by the amount of generated electrons and will grow at the rate proportional to G,

$$\left[\frac{dV}{dt}\right]_{\tau_d\lesssim t<\tau_M}\approx\frac{NeGd^2}{2\epsilon}\ . \tag{37}$$

At this rate, a polarization voltage of magnitude given by Eq. (1) will be reached in time $t=\tau_M$, when the motion of holes can no longer be neglected. The magnitude of the transient polarization is clearly limited by

$$V_{\text{trans}}^{\max}\approx\frac{dV}{dt}\tau_M=\frac{NGd^2}{2\mu_hp_0}\ , \tag{38}$$

which is similar in form to Eq. (1). The difference is that the voltage (37) is not subordinated to Eq. (2), so that $V_{\text{trans}}^{\max}$ retains the same value even as $\tau_e\to\infty$. Therefore, if $G>p_0/\tau_e$, then the evolution of the polarization will show transient peaks. However, we shall assume $G<p_0/\tau_e$, since as discussed above, higher values of G do not lead to a higher steady-state polarization. In this

case, the transient voltage can be expected to show no peaks. Figure 3(a) qualitatively illustrates both limits of the transient behavior of the photovoltage.

On the trailing side of the pulse, the decay of the polarization will also occur over a characteristic time of order τ_M or τ_d, whichever is longer. Consider for concreteness the sawtooth superlattice, Fig 2(a). Transient processes occur when the steady-state balance (3) of the currents J_e and J_h is temporarily violated. After the light is shut off, the minority concentration n is emptied (as electrons travel downhill) over most of the period d and the electron current is eliminated. Only near the sawtooth bottom will the rate be still controlled by a slower τ_e, but this lagging residual recombination process can be expected to have only a minor effect on the photovoltage. Rapid elimination of electrons from the sawtooth slopes will have a consequence, similar to the transient effect on the leading edge of the pulse. If $\tau_d \ll \tau_M$, then for a period of time δt ($\tau_d \lesssim \delta t \ll \tau_M$) the photopolarization voltage will decay at the rate given by Eq. (37)—with an opposite sign. For $G > p_0/\tau_e$, the transient voltage δV_1 may even be opposite in sign to the steady state V_1. At any time during the transient period, the surface density of charge $\delta\sigma(t)$ giving rise to $\delta V_1(t)$ can be estimated from Gauss's law, $|\delta\sigma| \approx \epsilon \delta V_1/d$. The net current density δJ, flowing during δt, is that of a p-type conductor driven by the field $\delta V_1/d$, i.e., $\delta J = \delta V_1 e\mu_h p_0/d$. This current will discharge the polarization in time $\delta t \approx \delta\sigma/\delta J = \tau_M$.

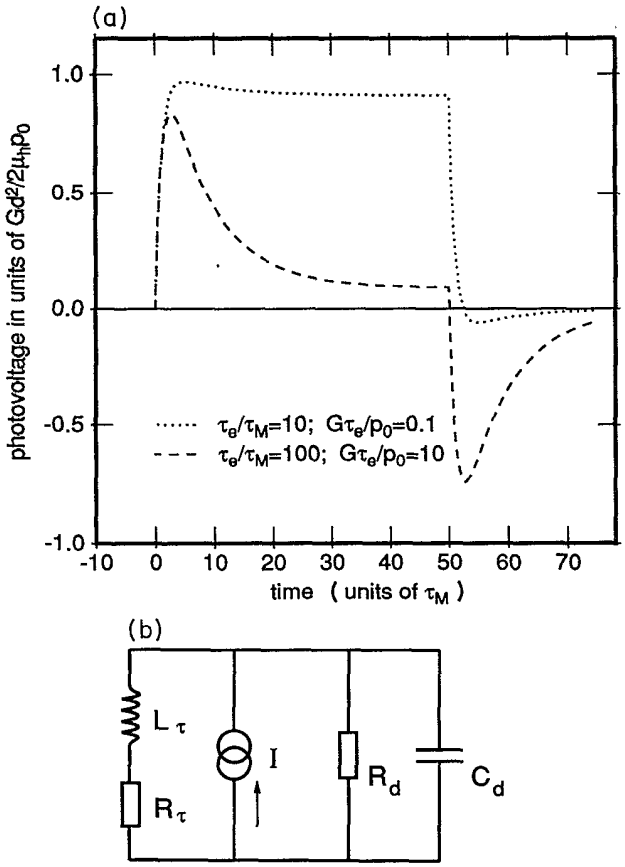

FIG. 3. Transient response of the photopolarization effect. (a) Evolution of the photovoltage per superlattice period, excited by a rectangular light pulse of duration $\tau_p = 50\tau_M$ in two limits: $G \gg p_0/\tau_e$ and $G \ll p_0/\tau_e$. (b) Equivalent circuit model employed in the calculation of (a).

Neglecting the transient overshoots, the onset and the dielectric relaxation of the photopolarization in each period can be modeled by an equivalent circuit consisting of a current source $I(t)$, a capacitor C_d, and two resistors, R_d and R_τ, defined (for a device of area A) by

$$C_d = \frac{\epsilon A}{d}\,, \qquad R_d = \frac{d}{e\mu_h p_0 A}\,, \qquad R_\tau = \frac{R_d p_0}{G\tau_e}\,, \tag{39}$$

so that $R_d C_d = \tau_M$ equals the Maxwell relaxation time (34). The current source produces

$$I = Ad^{-1}\int [-J_e(x)]dx \approx AeGd/2$$

when the light is on, and $I = 0$ otherwise. The transient overshoot effect can be included by adding into the R_τ branch of the circuit an inductance $L_\tau = \tau_e R_\tau$. Our equivalent circuit model of one superlattice period is illustrated in Fig. 3(b). Plots illustrating the time evolution of the photopolarization, shock excited by a rectangular light pulse [Fig. 3(a)], have been actually computed for this circuit, using the standard Laplace transform techniques.[7]

It should be emphasized that our circuit model does not contradict the experimental observation[1] that the duration of the transient effect is independent of τ_e. Indeed, under the condition $G\tau_e \gg p_0$, realized in the experiment, the model predicts that the transient peak decays with a characteristic time $\tau \approx p_0/G \ll \tau_e$. On the other hand, in the regime $G\tau_e \ll p_0$ (a regime that has not been investigated experimentally but is of interest to us), the decay of the transient peak is characterized by $\tau \approx \tau_e$ but the relative magnitude of the peak itself is of the order $G\tau_e \ll p_0$ and can be neglected.

B. Device under load

Let us now discuss what happens when a photopolarized structure is loaded by an impedance Z_L. First, consider the situation when the device is shorted by a resistor R_L. If the structure contains internal barriers, like in Fig. 2(b), then (assuming an effectively infinite barrier resistance R_b) only a transient current can flow. This current will transfer a charge δQ between the top and the bottom cladding layers of the superlattice and ensure that the overall voltage drop on R_L will vanish in the steady state. A small redistribution of charge of order δQ will occur in every period, resulting in an electric field in the barrier separators that exactly cancels the photogenerated voltage V_1, as illustrated in Fig. 4(a). The transferred charge δQ is evidently determined by the condition

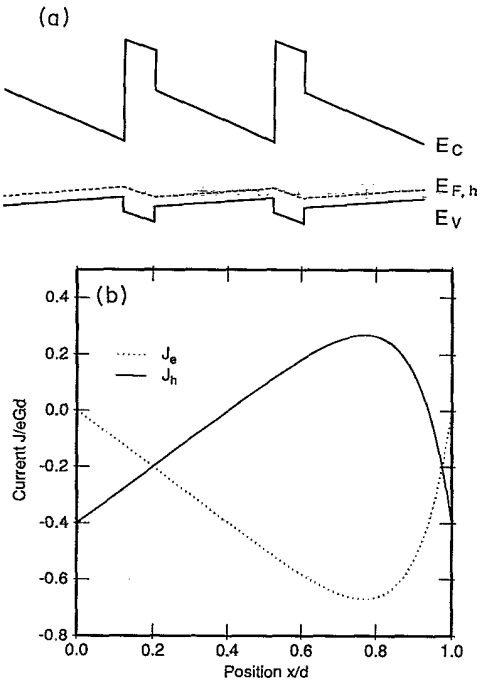

FIG. 4. Photopolarized superlattice under load. (a) Structure with barrier separators under a resistive load. (b) Electron and hole current-density profiles in a shorted sawtooth superlattice.

$NV_1=(\delta Q/\epsilon A)Nb$, where b is the thickness of a single barrier. Thus, the photopolarized superlattice with internal barrier separators behaves as an element with a resistance $R_b^{\rm tot}=NR_b$ and a capacitance $C_b^{\rm tot}=C_b/N$, where

$$C_b=\frac{\epsilon A}{b} . \tag{40}$$

In the absence of barrier separators (or for a finite $R_b^{\rm tot}$), an external dc current $I_L=V/R_L$ flows through the load in the direction opposite to the photogenerated hole current. Therefore, in Eq. (16) we must replace $J_h=-J_e$ by $\tilde{J}_h=J_h-V/R_L$, and the photovoltage per period will decline to $\tilde{V}_1=V_1-I_LR_d$. On the other hand, it is obvious that $V=N\tilde{V}_1-I_LR_b^{\rm tot}$, whence we find

$$V=\frac{NV_1R_L}{R_{\rm int}+R_b^{\rm tot}+R_L} , \tag{41}$$

where $R_{\rm int}\equiv NR_d$. Consider, for example, a shorted sawtooth superlattice: $R_L=R_b^{\rm tot}=0$. In this case, we find $I_L=V_1/R_d$ and $V=\tilde{V}_1=0$. Figure 4(b) displays the distribution of currents $J_e(x)$ and $J_h(x)$ in a single period of a shorted photopolarized sawtooth superlattice, calculated from Eq. (15).

Similar analysis is easy to carry out for a capacitive load C_L. For a structure without barrier separators (or any finite R_b) under dc conditions, this situation is equivalent to an open circuit. On the other hand, for a photopolarized structure with insulating internal barriers, $R_b=\infty$, this situation leads to a partial transfer of the polarization charge to the load capacitor. The transferred charge, δQ, will raise the voltage on the load to $V=\delta Q/C_L$, while the charge $(-\delta Q)$ will induce an electric field across the internal barriers that partially cancels the photogenerated voltage. It is easy to see that this results in lowering the voltage from NV_1 to

$$V=\frac{NV_1C_b^{\rm tot}}{C_b^{\rm tot}+C_L} . \tag{42}$$

Thus, under dc conditions, loading the device with internal barriers by a large capacitor, $C_L\gg C_b^{\rm tot}$, is equivalent to a short.

C. Equivalent circuit

The behavior of the photopolarized superlattice described above for several limiting cases can be modeled by an equivalent circuit, shown in Fig. 5. Elements of this circuit, C_b, R_d, R_τ, and C_b, are given by Eqs. (39) and (40) and R_b is determined by the tunneling of thermionic transport of holes through the barrier separators. The model current source is assumed to deliver a current $I=I[G(t)]$, such that $IR_d=V_1$. In other words, this current equals the average steady-state electron current of the superlattice under illumination

$$I(t)=\frac{A}{d}\int_0^d[-J_e(x)]dx . \tag{43}$$

The time dependence of I arises through the dependence of $J_e(x)$ on $G(t)$. In the instance of a sawtooth superlattice, $I(t)\approx AeG(t)d/2$. The model circuit of Fig. 5 is adequate for treating not only the steady state but also the transient processes after a change of either the load or the illumination intensity, provided we are considering these processes on the time scale longer than τ_M.

In practice, it will be convenient to lump similar elements from different periods together. The equivalent circuit for the entire superlattice, consisting of N periods, will have the same structure as a single period of the circuit in Fig. 5, but with the elements modified according

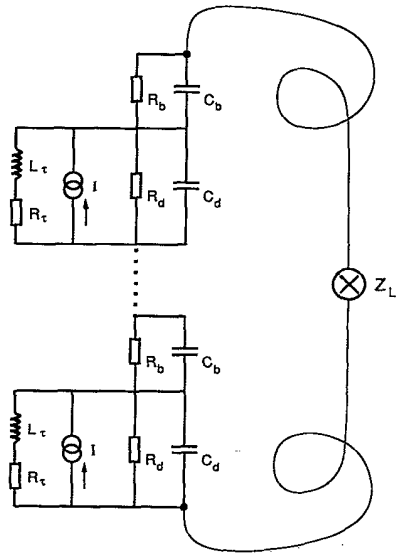

FIG. 5. Equivalent circuit of a loaded photopolarizable superlattice.

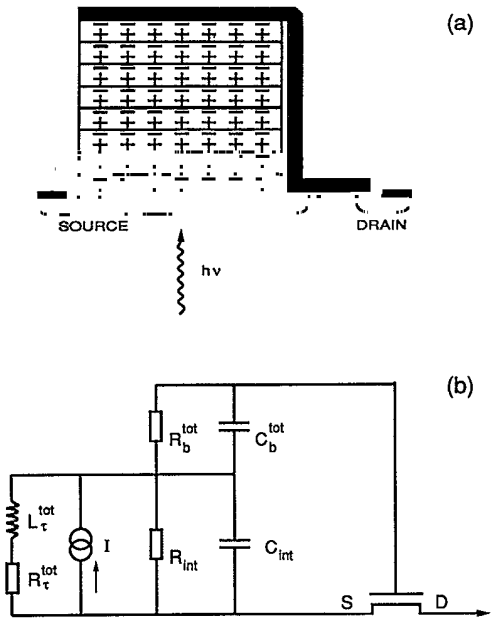

FIG. 6. Integration of a photopolarization detector with a FET. (a) Schematic cross section. (b) Equivalent circuit.

to the following rule:

$$C_d \rightarrow C_{\text{int}}, \quad R_d \rightarrow R_{\text{int}},$$
$$C_b \rightarrow C_b^{\text{tot}}, \quad R_b \rightarrow R_b^{\text{tot}},$$
$$L_\tau \rightarrow L_\tau^{\text{tot}}, \quad R_\tau \rightarrow R_\tau^{\text{tot}},$$

with no modification in the current source. The new elements are given by

$$C_{\text{int}}=C_d/N, \quad R_{\text{int}}=NR_d,$$
$$C_b^{\text{tot}}=C_b/N, \quad R_b^{\text{tot}}=NR_b, \tag{44}$$
$$L_\tau^{\text{tot}}=\tau_e R_\tau^{\text{tot}}, \quad R_\tau^{\text{tot}}=NR_\tau.$$

An example of the use for this circuit will be presented below [Fig. 6(b)].

IV. INTEGRATION WITH A FIELD-EFFECT TRANSISTOR

The polarizable superlattice detector is naturally suited for an integration with an FET amplifier. Because the input of an FET is capacitive, it draws no current from the superlattice, except in transient. Therefore, both the conducting superlattices and those with internal barrier separators can be used. In the following, we shall assume a conducting sawtooth superlattice, as in Fig. 2(a) or 2(c), with the understanding that the results can be extended to the case with internal barriers, using Eq. (42).

Consider the small-signal response of an integrated-detector–FET pair, illustrated in Fig. 6, to a time-varying illumination, $\delta G(t)=\alpha\delta\Phi(t)$. It will be assumed that the bandwidth of δG is less than $1/\tau_M$ so that the equivalent circuit of Fig. 5 can be employed. Let us first discuss the efficiency of the integrated detector, defined as the number of electrons flowing through the drain of the FET per photon incident on the superlattice

$$\eta \equiv \frac{e^{-1}\delta I_{\text{out}}}{A\delta\Phi} . \tag{45}$$

The steady-state voltage V_g on the gate of the FET is given by

$$V_g = I(G)\frac{R_{\text{int}}R_\tau^{\text{tot}}(G)}{R_{\text{int}}+R_\tau^{\text{tot}}(G)} , \tag{46}$$

whence we find, using Eqs. (39), (43), and (44)

$$\delta V_g \equiv \frac{\partial V_g}{\partial G}\delta G = \frac{\delta I R_{\text{int}}}{(1+G\tau_e/p_0)^2} . \tag{47}$$

For a sawtooth superlattice, assuming $G\tau_e/p_0 \ll 1$, we have

$$\delta V_g \approx \delta I R_{\text{int}} \approx \frac{Gd^2}{2\mu_h p_0} . \tag{48}$$

Let the transconductance g_m of the FET be related to the superlattice conductance $1/R_{\text{int}}$ by a factor M,

$$g_m R_{\text{int}} = M . \tag{49}$$

Since $\delta I_{\text{out}}=g_m\delta V_g$, we obtain from (48)

$$\eta = M\alpha d/2 . \tag{50}$$

It is clear that the orientation of the polarization field can be designed to point up or down, corresponding to two possible orientations of an asymmetric superlattice. Therefore, the sign of η is at the designer's disposal: For the same type of conductivity in the FET, one can have the current either *increasing* or *decreasing* with the illumination.

Next, we consider the response time τ. From the equivalent circuit we find

$$\tau = \tau_g(M+1)+\tau_M , \tag{51}$$

where $\tau_g \equiv C_g/g_m$ is the small-signal gate delay and C_g the gate capacitance of the FET. The tradeoff between the efficiency and the speed of response, expressed by Eq. (51), is quite obvious: for taking advantage of a high gain $M>1$ in Eq. (50), we pay the price of degrading the $R_{\text{int}}C_g$ time constant.

Parameters that determine M are seen from the following expression:

$$M = N\frac{\tau_M}{\tau_g}\frac{d}{d_g}\frac{\epsilon_g A_g}{\epsilon A} , \tag{52}$$

where A_g, d_g, and ϵ_g are, respectively, the gate area and the thickness and the permittivity of the gate dielectric. The total active thickness of the superlattice Nd is obviously limited by the absorption length α^{-1}. Substituting α^{-1} for Nd in Eq. (52) and using (50), we have

$$\eta = \frac{d}{2d_g}\frac{\epsilon_g A_g}{\epsilon A}\frac{\tau_M}{\tau_g} . \tag{53}$$

As an example, suppose we are employing a state-of-the-art FET with an intrinsic gate delay $\tau_g = 5$ ps and a superlattice characterized by $\alpha d = 0.1$ and $\tau_M = 1$ psec, both very reasonable numbers. The optimum number of period is $N \approx 10$. The integrated device will have an intrinsic response time $\tau \approx 10$ psec at $\eta \approx 5\%$ and $\tau \approx 200$ psec at $\eta \approx 100\%$. Optimization of the device toward either the faster or the more efficient mode can be done on the basis of Eq. (53).

As suggested by Eq. (47), a small-signal operation of the device at low illumination levels does not require a particularly short minority lifetime τ_e. Such a requirement will arise, however, from noise considerations that go beyond the scope of the present work. Qualitatively, the situation can be clarified by looking at a large-signal "digital" operation of the integrated pair. Such an operation requires a large on-off ratio in the output current, and therefore the swing δV_g must be sufficiently large, e.g., $\delta V_g \gg kT$. Using Eq. (47), we see that this implies a requirement

$$\tau_e \ll \frac{d^2}{2\mu_h}\frac{e}{kT} . \tag{54}$$

Thus, at room temperature, taking $d \lesssim 2000$ Å and $\mu_h \gtrsim 50$ cm^2/V sec, we need $\tau_e \ll 10^{-10}$ sec. Such short lifetimes should be achievable with the radiation damage techniques[3-5] or by a controlled low-temperature molecular-beam epitaxy.[8] Another interesting possibility in this context will be discussed in the next section.

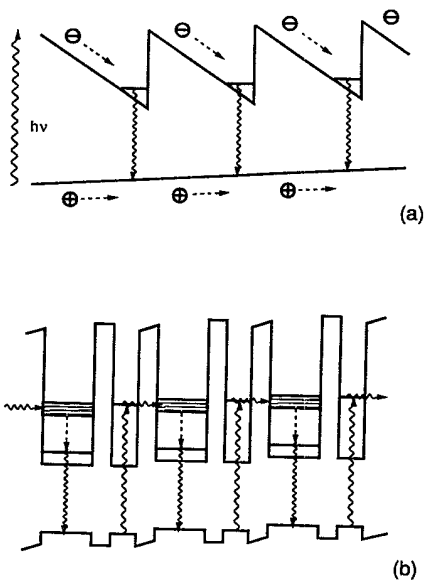

FIG. 7. Possible exotic schemes: (a) stimulated emission at the long-wavelength part of the period, and (b) multiple double-quantum-well superlattice.

V. QUANTUM VARIATIONS

Elsewhere in this paper our consideration was restricted to essentially classical processes: the drift-diffusion transport of carriers and their classical interaction with light. In this section, we discuss two quantum variations on our main theme, which is the photopolarization effect in asymmetric superlattices. The first of these variations involves *stimulated recombination.*

As is well known, the radiative recombination rate can be dramatically enhanced by the stimulated emission process. Consider a photopolarizable superlattice placed in a resonant cavity for the radiation of wavelength corresponding to the narrow-gap end of the superlattice period, Fig. 7(a). Such a cavity can be formed between two cleaved facets, like in a conventional edge-emitting laser, or between two planar quarter-wave dielectric mirror stacks, like in optically pumped vertical-cavity surface-emitting lasers.[9] Subject to an optical pumping G above the lasing threshold level, the electrical behavior of this structure will be similar to that considered in Sec. II B, with τ_2 given by the stimulated radiative lifetime τ_r^{st}, which can be as short as 10^{-13} sec.

The photogenerated voltage in this case will be quite accurately described by Eq. (25), but the restriction (26) will not be a practical limitation. Taking exemplary parameters $d = 2000$ Å, $p_0 = 10^{17}$ cm^{-3}, and $\mu_h = 50$ cm^2/V sec, we find that for the generation rate $G \approx 10^{27}$ cm^{-3} sec^{-1} (corresponding to an incident power of 10 kW/cm^2 and an absorption coefficient $\alpha \approx 10^4$ cm^{-1}) the photovoltage is about 40 mV per superlattice period, well below the limit set by (26). At the shortest τ_r^{st}, a practical limit will likely be set by the overall height of a sawtooth slope or, for castellated superlattices, by the temperature $eV_1^{max} \lesssim \Delta + kT$.

Under a time-varying optical pumping, described by an excitation function $G_0 + \delta G(t)$, the structures of Fig. 7(a) will produce a synchronous combination of the optical and the electrical outputs, both faithfully tracking $\delta G(t)$ up to the bandwidths in terahertz range. Such a device may find applications in optical communication systems. Moreover, the wavelength of the optical output itself may be controllable to some extent by the intensity of the base pumping level G_0. This effect can be expected to occur due to the Stark shift by the polarization field of the ground electronic energy level in a sawtooth superlattice.

Our second quantum variation involves *tunneling transport.* Consider a superlattice whose period consists of two quantum wells, one narrow and the other wide, see Fig. 7(b). The superlattice is doped p type. Under certain conditions, it is possible to achieve a strong asymmetry between the wells in either the absorption rate or the recombination lifetime (or both of these quantities). An example of such a situation has been considered in Refs. 10 and 11, where the interest is focused on the transient luminescence and polarization oscillations upon an ultrashort generation pulse. Those transient effects, arising from the Rabi oscillations of electrons between the two wells, decay after a short phase-relaxation time, analogous to the T_2 of nuclear magnetic resonance. It has been pointed out[11] that the steady state, arising after the Rabi oscillations have relaxed, corresponds to a polarized

superlattice, but from the perspective of the present work that state is still "transient"—to be screened by the motion of holes. Inasmuch as we are not interested here in the transient oscillations (and hence a long T_2 is not required), we can substantially simplify the scheme for establishing the asymmetric absorption that gives rise to the internal steady-state current and the polarization voltage. For example, this can be done as follows.

Suppose the first excited energy level of electrons in the wide well is degenerate with the ground level in the narrow well. Optical transitions in the wide well can be suppressed if the linewidths $\hbar\Delta\omega$ of the incident radiation is narrower than the lifetime-limited width Γ of the second energy level in the wide-gap well. We assume that the level broadening $\Gamma \equiv \hbar/\tau_c$ is caused by intersubband scattering and is about 10 meV, a typical number. Broadening of the ground level in the narrow well, on the other hand, is mainly due to the finite lifetime τ_t against the escape from the well by tunneling into the wide well. That broadening is assumed to be of the order of the excitation linewidth, i.e., $\Delta\omega\tau_t \sim 1$ and much smaller than the collision broadening of the wide-well level, i.e., $\tau_t \gg \tau_c$.

Under these conditions, the optical absorption in the wide well is suppressed compared to that in the narrow well by a factor $\Delta\omega\tau_c = \tau_c/\tau_t \ll 1$, and hence illuminating the system with a monochromatic light, tuned to the fundamental transition in the narrow well, will mainly generate electron-hole pairs in that well. In the regime $\tau_c \ll \tau_t$, the tunneling rate is practically independent of the actual alignment of the two levels, so long as the narrow level falls within the band Γ of the broad level. Even if the recombination times in the two wells are equal, the asymmetry in the absorption rate will cause an effect of polarization. The magnitude of this effect depends on the barrier resistance of the hole transport and can be tuned in a wide range. To a reasonable approximation, this situation can be described by the equivalent circuit of Sec. III and Eq. (39), where d should now be taken as the separation between the centroids of the electronic wave functions in the two wells, and μ_h the mobility of holes perpendicular to the superlattice.

The coupled-well scheme admits of many further variations, including the design of disparate recombination times in the two wells, the use of stimulated recombination in a resonant cavity, etc. In the limit of extremely short recombination time in the wide well, e.g., provided by the stimulated emission in a resonant cavity, the photovoltage generated per period is limited by the width Γ because further voltage would detune the tunneling resonance. However, the number of periods can be quite large and polarization voltages of order 1 V seem to be within reach. The response time of the tunneling photopolarization is determined by τ_t and can be well in the subpicosecond range before violating the inequality $\tau_c \ll \tau_t$.

VI. CONCLUSION

We have described a steady-state photogalvanic effect in superlattices lacking reflection summetry. The effect arises when the photogenerated minority carriers, prior to their recombination with the majority carriers, are transported by a built-in field within the superlattice period, so that the median sites for the generation and recombination are displaced from one another. In the steady state, this requires an internal current of majority carriers and a voltage driving that current. The resultant polarization of the superlattice is a tangible effect, provided the minority carrier lifetime is sufficiently short, and it can be used to control the gate of a field-effect transistor.

The described effect is likely to generate useful applications. One of its advantages lies in the intrinsic speed of response, which is essentially limited by the dielectric relaxation time and controlled by the majority-carrier conductivity. For an integrated system, consisting of the proposed superlattice detector and a FET, the response time can be made as short as $2\tau_g$, where τ_g is gate delay of the FET. The fundamental tradeoff between the speed and the efficiency of such an integrated system is discussed in Sec. IV. An interesting practical advantage of the proposed scheme is that the FET output can be either in phase or 180° out of phase with the light input, depending on the orientation of the asymmetric superlattice.

Another practical advantage of the proposed effect is its expected tolerance to material imperfections. The key design requirement for the efficient and fast operation is a short minority lifetime, a property promoted by certain crystal defects and impurities. It is, therefore, likely that some of the structures described in the present work can be implemented heteroepitaxially on lattice-mismatched foreign semiconductor substrates. One can envisage efficient and fast long-wavelength photodetectors, combined with GaAs or Si front-end amplifiers and integrated circuits on the same chip.

Finally, the effect lends itself to the implementation of a scheme, discussed in Sec. V, where the short lifetime is achieved not because of imperfections but owing to the stimulated recombination in a laser cavity. In this case, the device will generate the polarization voltage synchronously with the optical output, both modulated by the intensity of the optical pumping signal. The bandwidth of this modulation can be in the terahertz range. We believe the described effect will find important applications, especially for fiber-optic communications.

Note added in proof. An experiment, demonstrating the steady-state photovoltaic effect in asymmetrical graded superlattices, has been performed.[12] It shows an excellent agreement with Eq. (2), including the dependence on the minority-carrier lifetime. The observed photovoltaic response time (2 nsec) has been limited by an oscilloscope resolution.

[1]F. Capasso, S. Luryi, W. T. Tsang, C. G. Bethea, and B. F. Levine, Phys. Rev. Lett. **51**, 2318 (1983).

[2]H. Dember, Phys. Z. **32**, 554 (1931); W. Van Roosbroeck, J. Appl. Phys. **26**, 380 (1955).

[3]P. R. Smith, D. H. Auston, A. M. Johnson, and W. M. Augustinyak, Appl. Phys. Lett. **38**, 47 (1981).

[4]P. M. Downey and B. Schwartz, Appl. Phys. Lett. **44**, 47 (1984); P. M. Downey and B. Tell, J. Appl. Phys. **56**, 2672 (1984); P. M. Downey, R. J. Martin, R. E. Nahory, and O. G . Lorimo, Appl. Phys. Lett. **46**, 396 (1985).

[5]For comprehensive references see D. H. Auston, in *Semiconductors and Semimetals,* edited by R. B. Marcus (Academic, New York, 1990), Vol. 28.

[6]C. R. Crowell and S. M. Sze, Solid State Electron. **9**, 1035 (1966).

[7]G. Lancaster, *DC and AC Circuits,* 2nd ed. (Clarendon, Oxford, 1980).

[8]A. Y. Cho (private communication).

[9]D. G. Deppe, S. Singh, R. D. Dupuis, N. D. Gerrard, G. J. Zydzik, J. P. van der Ziel, C. A. Green, and C. J. Pinzone, Appl. Phys. Lett. **56**, 2172 (1990).

[10]S. Luryi, Solid State Commun. **65**, 787 (1988).

[11]S. Luryi, IEEE J. Quantum Electron. **27**, 54 (1991).

[12]C. T. Liu, J. M. Liu, P. A. Garbinski, S. Luryi, D. L. Sivco, and A. Y. Cho, Phys. Rev. Lett. **67**, 2231 (1991).